Supporting Information for

Co-seismic slip of the 18 April 2021 M_w 5.9 Genaveh earthquake in the South Dezful Embayment of Zagros (Iran) and its aftershock sequence

A. Mohammadreza Jamalreyhani[1,7*]
B. Léa Pousse-Beltran[2]
C. MirAli Hassanzadeh[3]
D. Samineh Sadat Arabi[4]
E. Eric A. Bergman[5]
F. Aref Shamszadeh[6]
G. Shiva Arvin[3]
H. Niusha Fariborzi[3]
I. Ali Songhori[7]

[1]GFZ German Research Center for Geosciences, Potsdam, Germany.

[2]University Grenoble Alpes, University Savoie Mont Blanc, CNRS, IRD, UGE, ISTerre, Grenoble, France.

[3]Department of Earth Sciences, Institute for Advanced Studies in Basic Sciences, Zanjan, Iran.

[4]SRBIAU Sience & Research Branch of Islamic Azad University

[5]Global Seismological Services, Golden, CO, USA

[6] Department of Earth Sciences, College of Sciences, Shiraz University, Shiraz, Iran

[7]Institute of Geophysics, University of Tehran, Tehran, Iran.

[*]Corresponding author: m.jamalreyhani@gmail.com

Text S1:

To investigate for possible trade-off between parameters during the uniform inversion we plot the results of the Monte Carlo restarts (Figures S8 and S9). For the NE-dipping fault, top and bottom depths are the most inter-dependent parameters, whereas others are not strongly showing trade-off between each other. Although top and bottom depths do not affect the geometry of the fault (dip, strike, position), therefore we are confident in the slip distributed fault model where we extended the fault plane. For the SW-dipping fault, slip and top depth as well as slip and bottom depth show interdependence. Although, as for the NE dipping fault, strike, dip and rake seem unaffected by trade-off. Therefore we are confident in the slip distributed fault model where distribution and slip are not inputs.

We conducted some additional tests in order to investigate further trade-off between slip and width. For that we repeated the uniform inversion by fixing the slip to an appropriate value for a Mw 5.9 earthquake, here 0.5 meters (see Table S5). If we compare with the inversions where all parameters are free, the inversions with fixed slip give higher RMS and Mw. In addition, when the slip is fixed, for the SW-dipping model, the dip is 7° higher (66°) and the fault plane is wider (top at 3.1 km and bottom at 9.9 km). For the NW-dipping fault model, solutions are similar.

To observe the influence of those parameters on the slip distribution model inversion of the SW-dipping model, we run a new inversion using a fault with a strike of 128°, dip of 59° and a rake of 94° (see Figure S10). We obtain a RMS of 0.00387 (vs 0.00384 for 69° dipping fault) and a slipping area constrained to 10.3 km and 3.4 km depth (vs 10.8 km and 3.6 km depth for 69° dipping fault). So here, the dip has a small influence on the depth distribution of the slip.

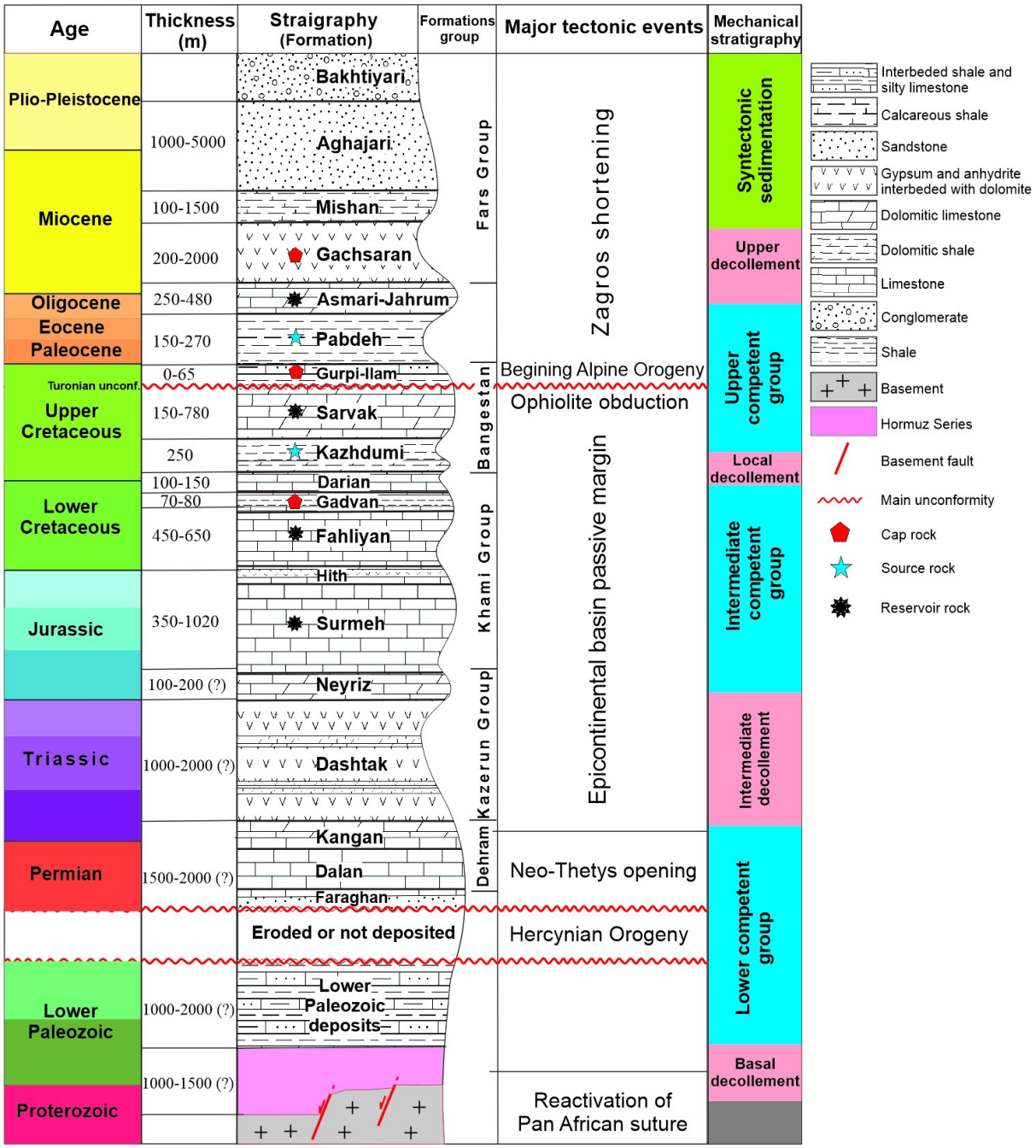

Figure S1; Stratigraphic column of the South Dezful Embayment based on surface and subsurface data (after Shamszadeh et al., 2022a).

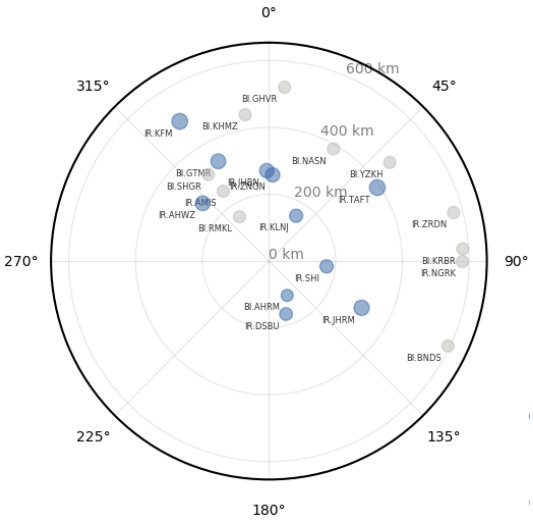
0°
45°
90°
135°
180°
225°
270°
315°
600 km
400 km
200 km
0 km
BI.GHVR
IR.KFM
BI.KHMZ
BI.NASN
BI.GTMR
BI.YZKH
BI.SHGR
IR.TAFT
IR.ZRDN
IR.AHWZ
IR.RMKL
IR.KLNJ
BI.KRBR
IR.NGRK
IR.SHI
BI.AHRM
IR.JHRM
IR.DSBU
BI.BNDS

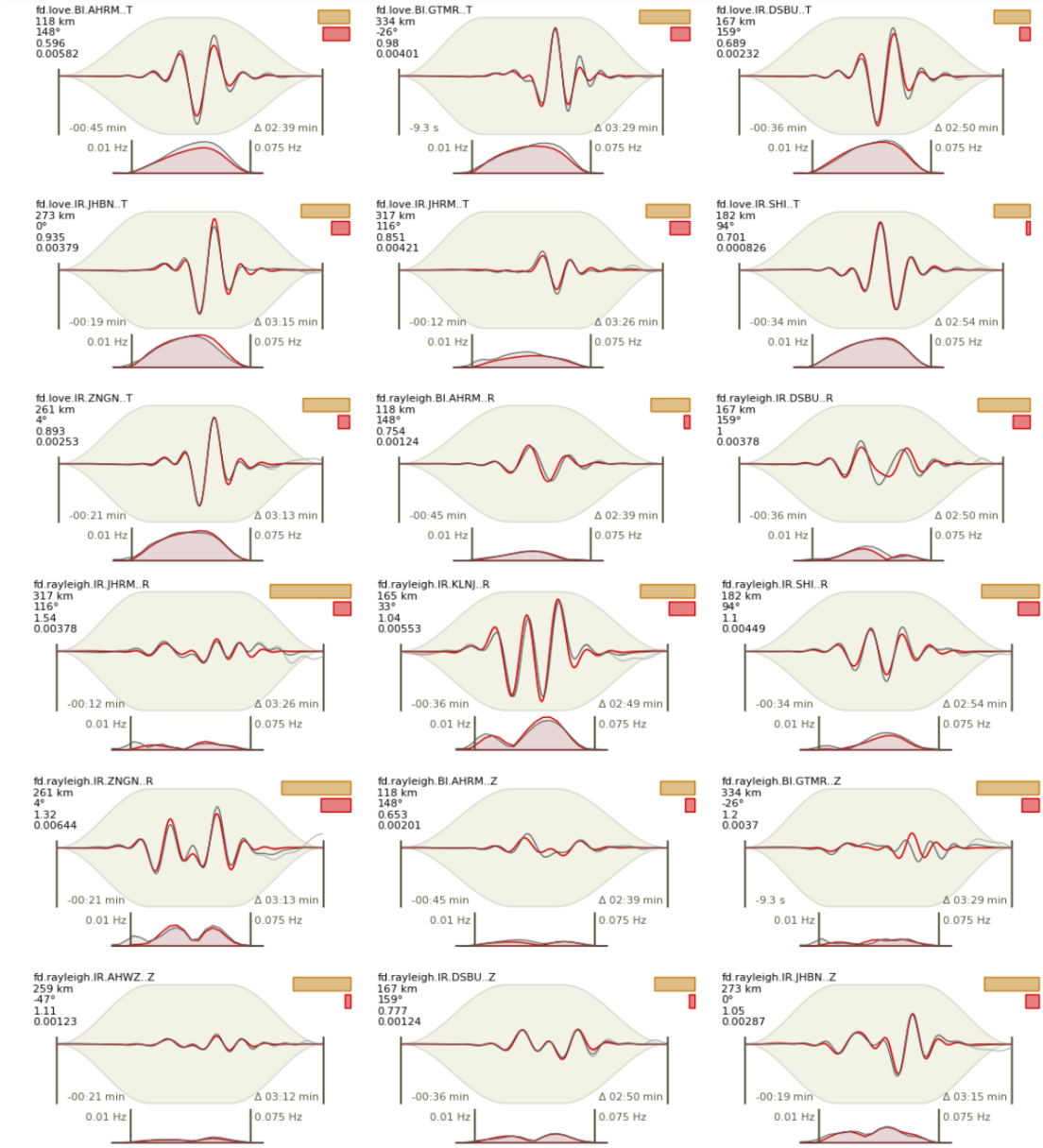
fd.love.BI.AHRM..T
118 km
148°
0.596
0.00582
fd.love.BI.GTMR..T
334 km
-26°
0.98
0.00401
fd.love.IR.DSBU..T
167 km
159°
0.689
0.00232
fd.love.IR.JHBN..T
273 km
0°
0.935
0.00379
fd.love.IR.JHRM..T
317 km
116°
0.851
0.00421
fd.love.IR.SHI..T
182 km
94°
0.701
0.000826
fd.love.IR.ZNGN..T
261 km
4°
0.893
0.00253
fd.rayleigh.BI.AHRM..R
118 km
148°
0.754
0.00124
fd.rayleigh.IR.DSBU..R
167 km
159°
1
0.00378
fd.rayleigh.IR.JHRM..R
317 km
116°
1.54
0.00378
fd.rayleigh.IR.KLNJ..R
165 km
33°
1.04
0.00553
fd.rayleigh.IR.SHI..R
182 km
94°
1.1
0.00449
fd.rayleigh.IR.ZNGN..R
261 km
4°
1.32
0.00644
fd.rayleigh.BI.AHRM..Z
118 km
148°
0.653
0.00201
fd.rayleigh.BI.GTMR..Z
334 km
-26°
1.2
0.0037
fd.rayleigh.IR.AHWZ..Z
259 km
-47°
1.11
0.00123
fd.rayleigh.IR.DSBU..Z
167 km
159°
0.777
0.00124
fd.rayleigh.IR.JHBN..Z
273 km
0°
1.05
0.00287
-00:45 min
Δ 02:39 min
-9.3 s
Δ 03:29 min
-00:36 min
Δ 02:50 min
-00:19 min
Δ 03:15 min
-00:12 min
Δ 03:26 min
-00:34 min
Δ 02:54 min
-00:21 min
Δ 03:13 min
-00:36 min
Δ 02:49 min
-00:21 min
Δ 03:12 min
0.01 Hz
0.075 Hz

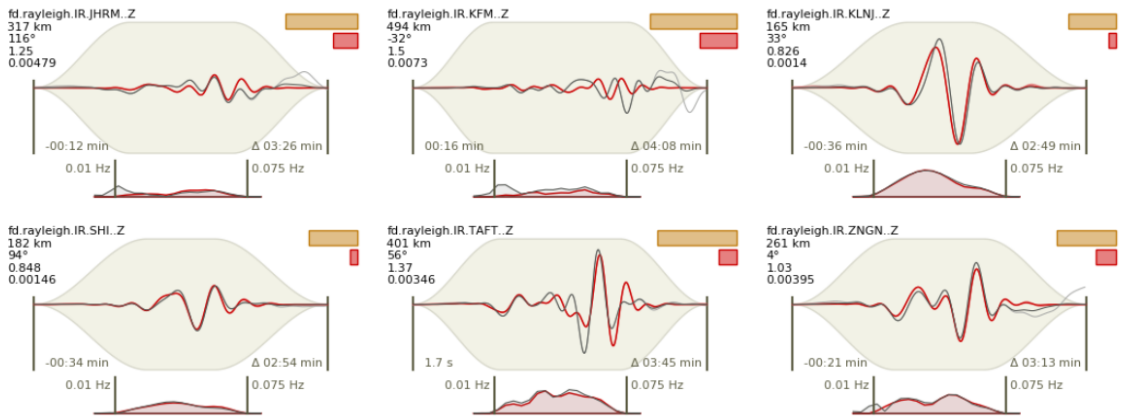

Figure S2, Station distribution and waveforms fitting in the time (Upper) and in the frequency (lower) domains for the 18 April 2021 Mw 5.9 Genaveh earthquake. Red and black waveforms/spectra show synthetic and observed records, respectively. Numbers within the panels describe the time window and the frequency band. Information to the left of each waveform gives (from top to bottom) the station name, component, distance to the source, and azimuth.

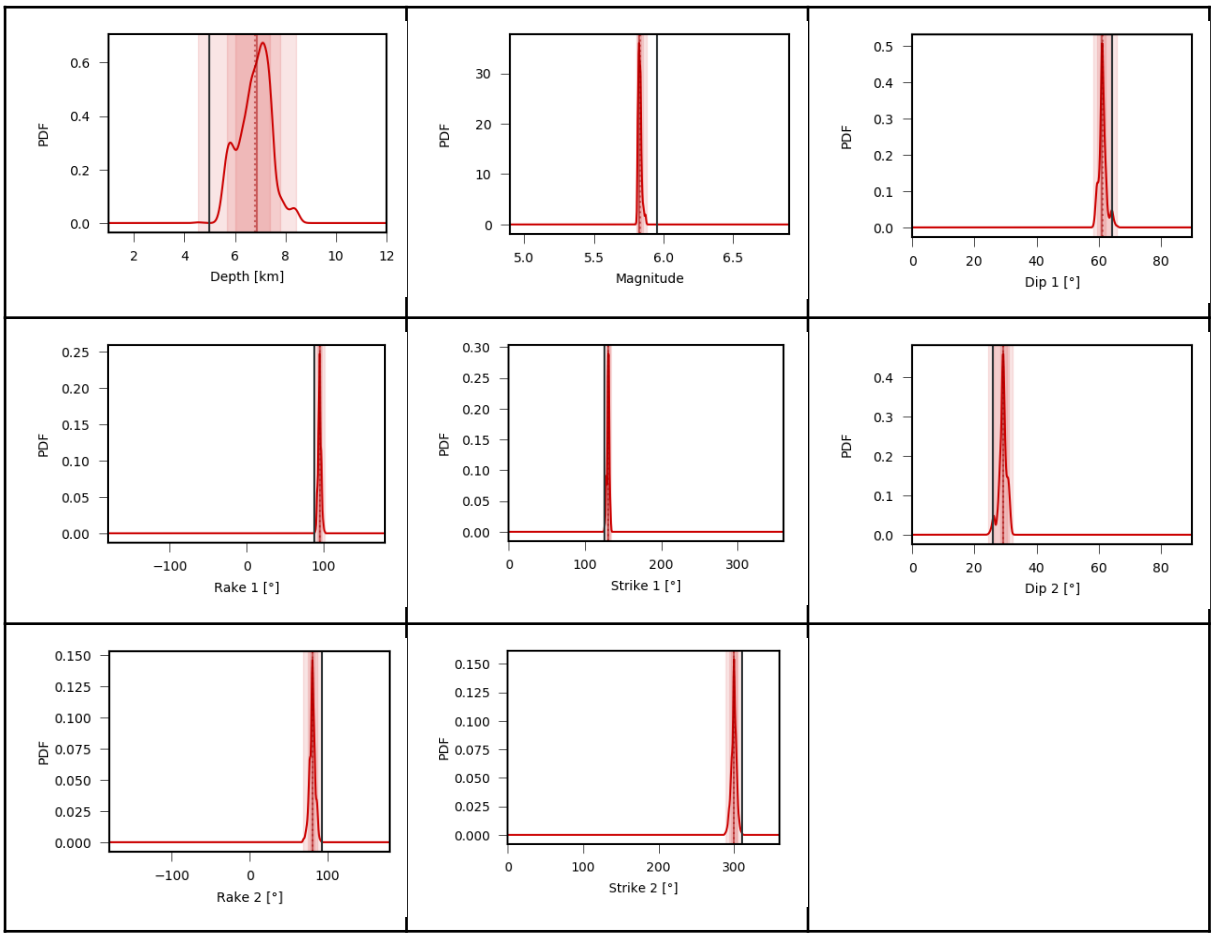

Figure S3, Probability density functions of the centroid depth and other source parameters obtained from waveform modeling for 18 April 2021 Mw 5.9 Genaveh earthquake. The plot ranges are defined by the given parameter bounds and (model space). The red solid vertical and dashed lines give the median and mean of the distribution, respectively. Dark gray vertical lines show initial values. The overlapping red-shaded areas show the 68% confidence intervals (innermost area), the 90% confidence intervals (middle area) and the minimum and maximum values (widest area).

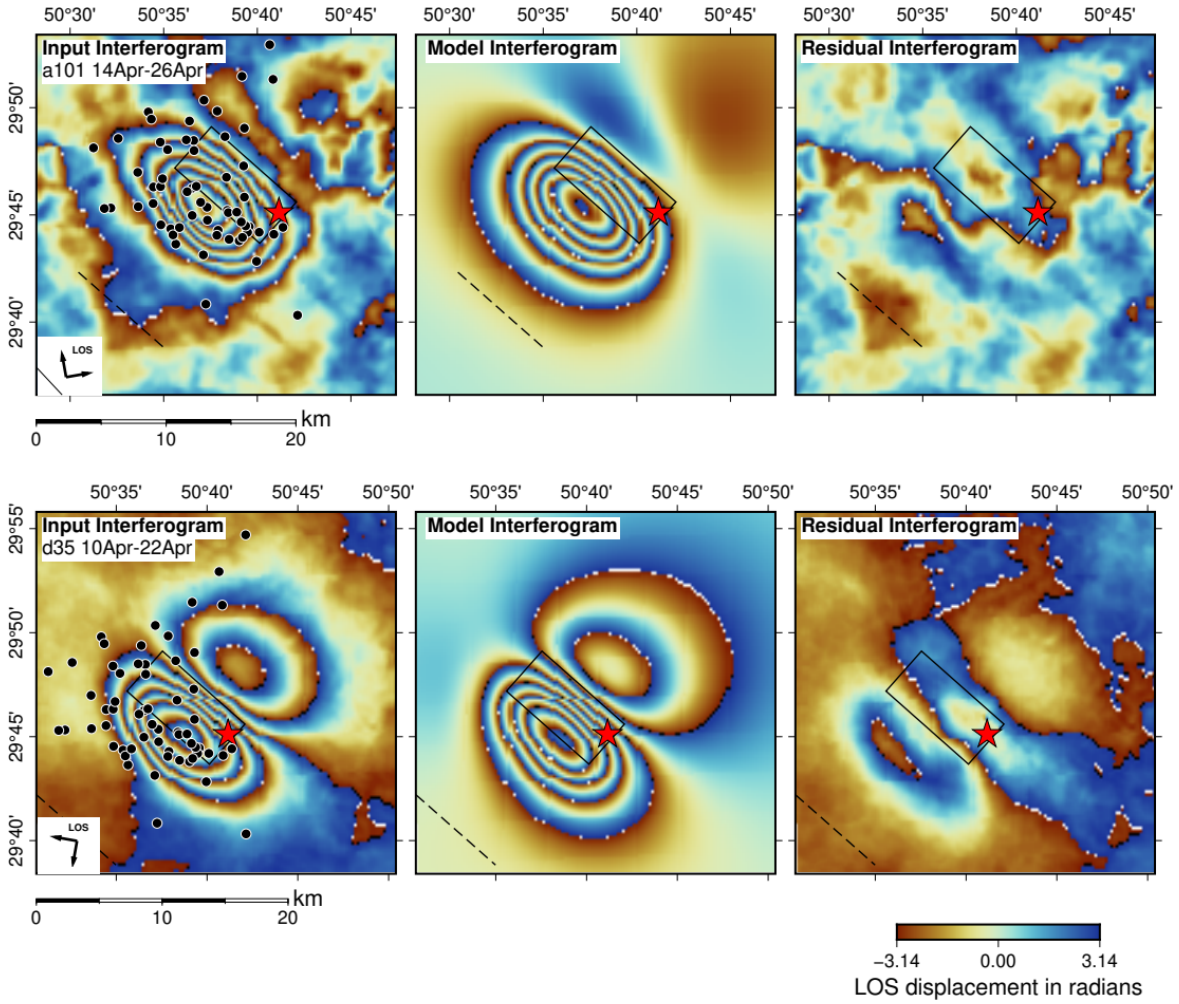

Figure S4, Uniform slip inversion result for NE-dipping fault model. The first and second row correspond, respectively, to the ascending track A101 and the descending track D35. From left to right columns : observed, model and residual interferograms. Results are shown re-wrapped. The dashed black line is the surface projection of the model fault, the black rectangle is the slipping model fault plane outline. Red star is the relocated epicenter of the mainshock. Black dots are the relocated aftershocks.

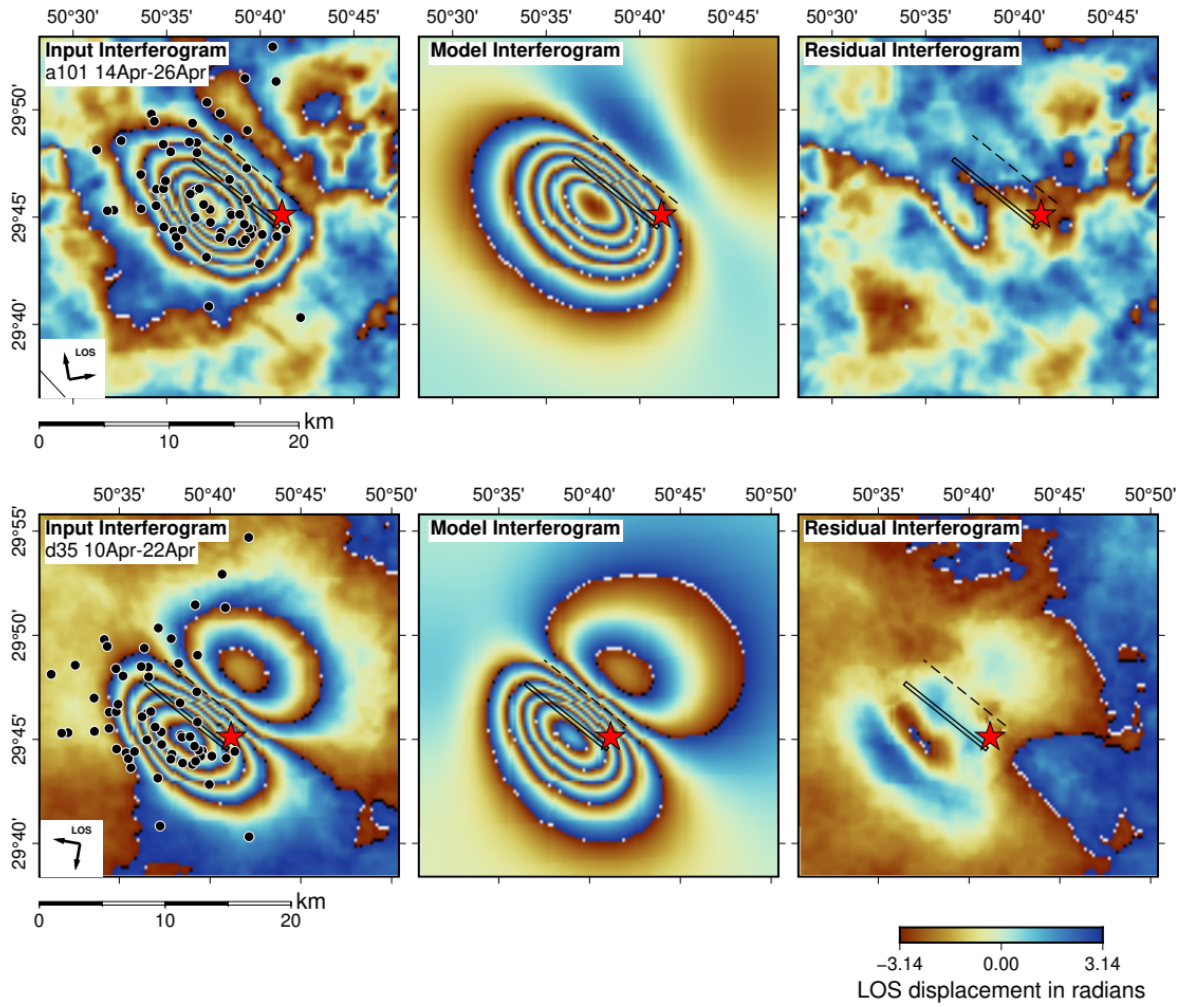

Figure S5, Uniform slip inversion result for SW-dipping fault model.The first and second row correspond, respectively, to the ascending track A101 and the descending track D35. From left to right columns : observed, model and residual interferograms. Results are shown re-wrapped. The dashed black line is the surface projection of the model fault, the black rectangle is the slipping model fault plane outline. Red star is the relocated epicenter of the mainshock. Black dots are the relocated aftershocks.

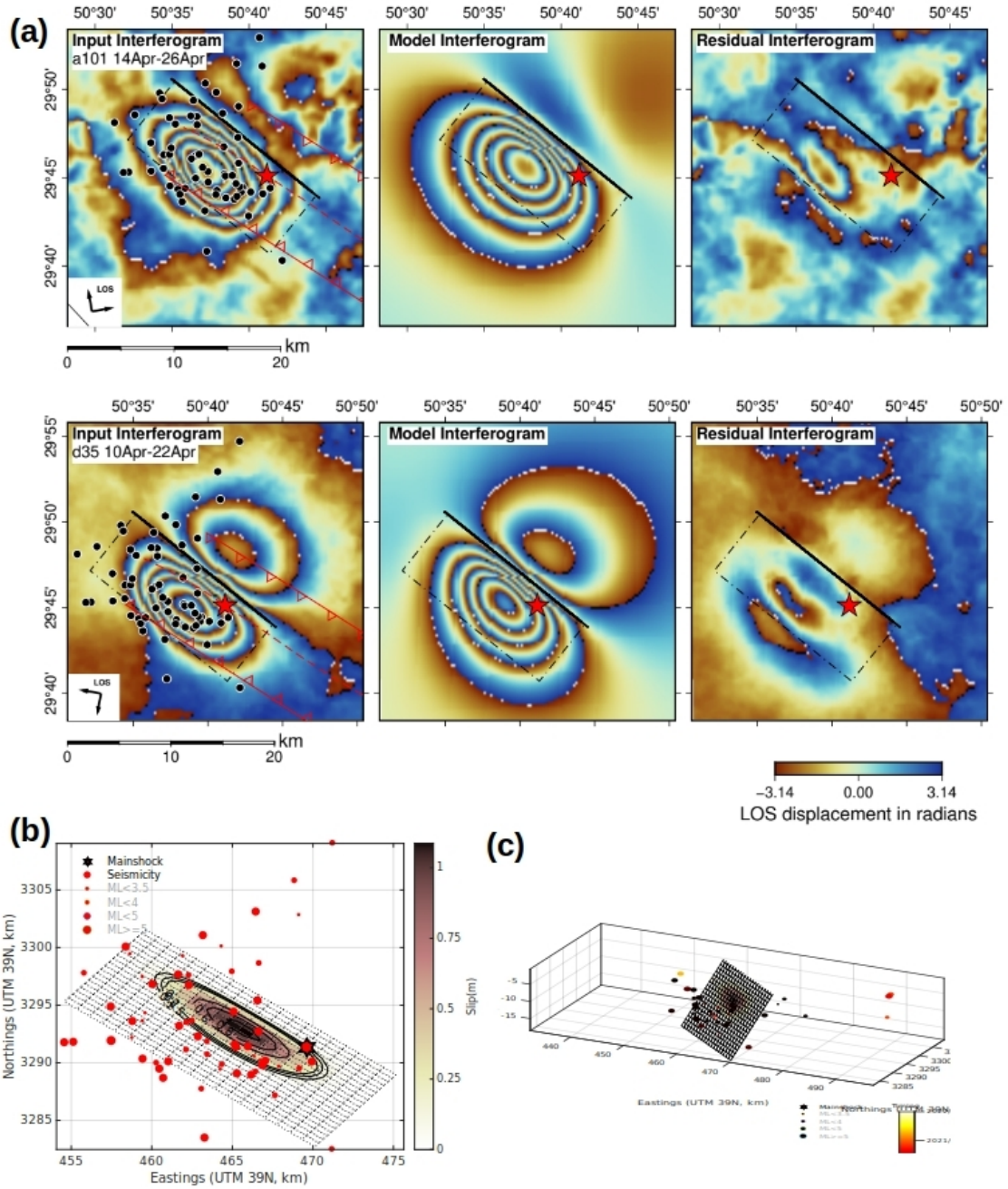

Figure S6, Coseismic slip distribution inversion results for SW-dipping fault model. (a) The first and second row correspond, respectively, to the ascending track A101 and the descending track D35. From left to right columns: observed, model and residual interferograms. Results are shown re-wrapped. The dashed black line is the surface projection of the model fault. Red star is the relocated epicenter of the mainshock. Black dots are the relocated aftershocks. The NW-SE trending blind thrust faults dipping NE and SW are shown by red lines. (b) Coseismic slip distribution in map view, the model fault is divided by a 1 km, 2 patch. The red star is the relocated epicenter, dots show the relocated aftershocks. (c) Coseismic slip distribution in 3D, dots show the relocated aftershocks colored according to time. The InSAR model moment reaches 1.138 × 1018 Nm (Mw 5.9). The model yields an RMS of 0.00384 m.

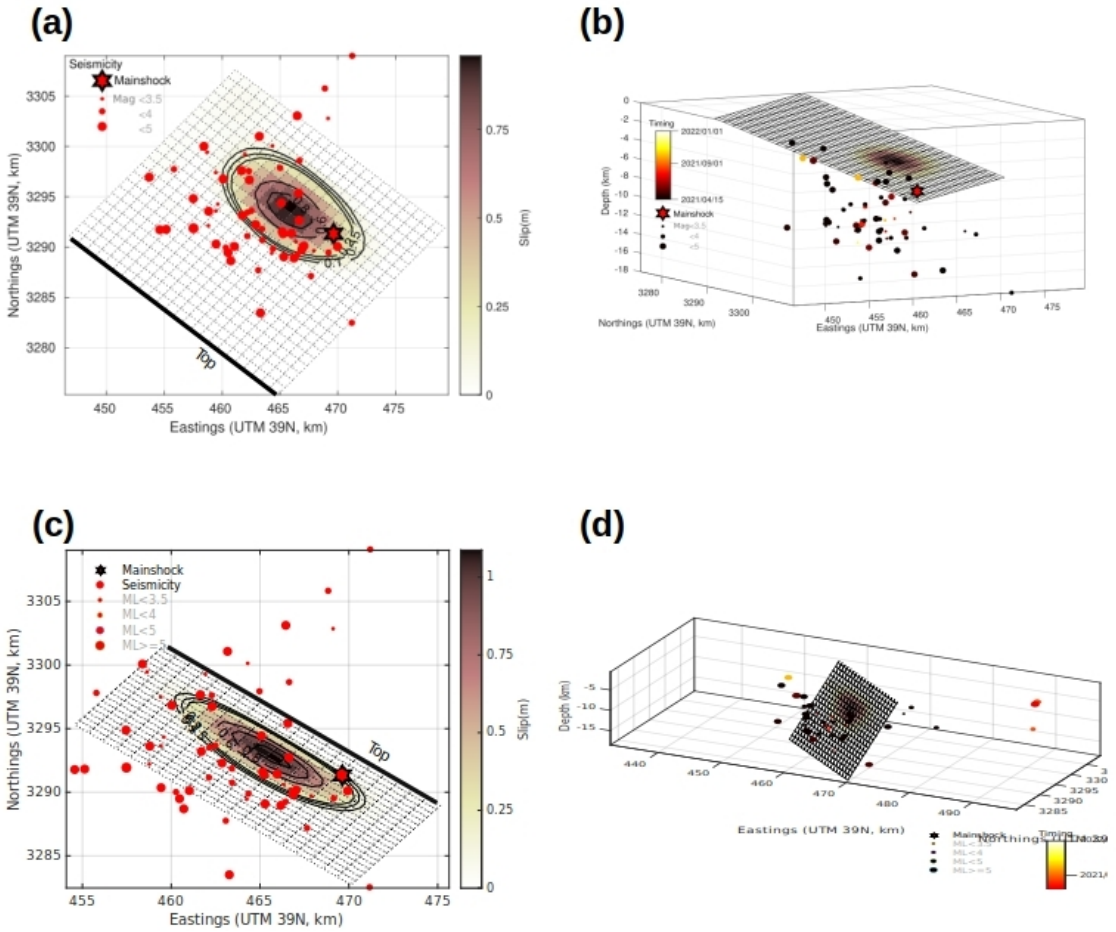

Figure S7, Comparison side by side of the two fault models; (a-b) NE-dipping fault model, (c-d) the SW-dipping fault model. (a) and (c) are the distributed slip contours in map view, the red star is the relocated epicenter, dots show the relocated aftershocks. (b) and (d) are the coseismic slip distribution in 3D, dots show the relocated aftershocks colored according to time.

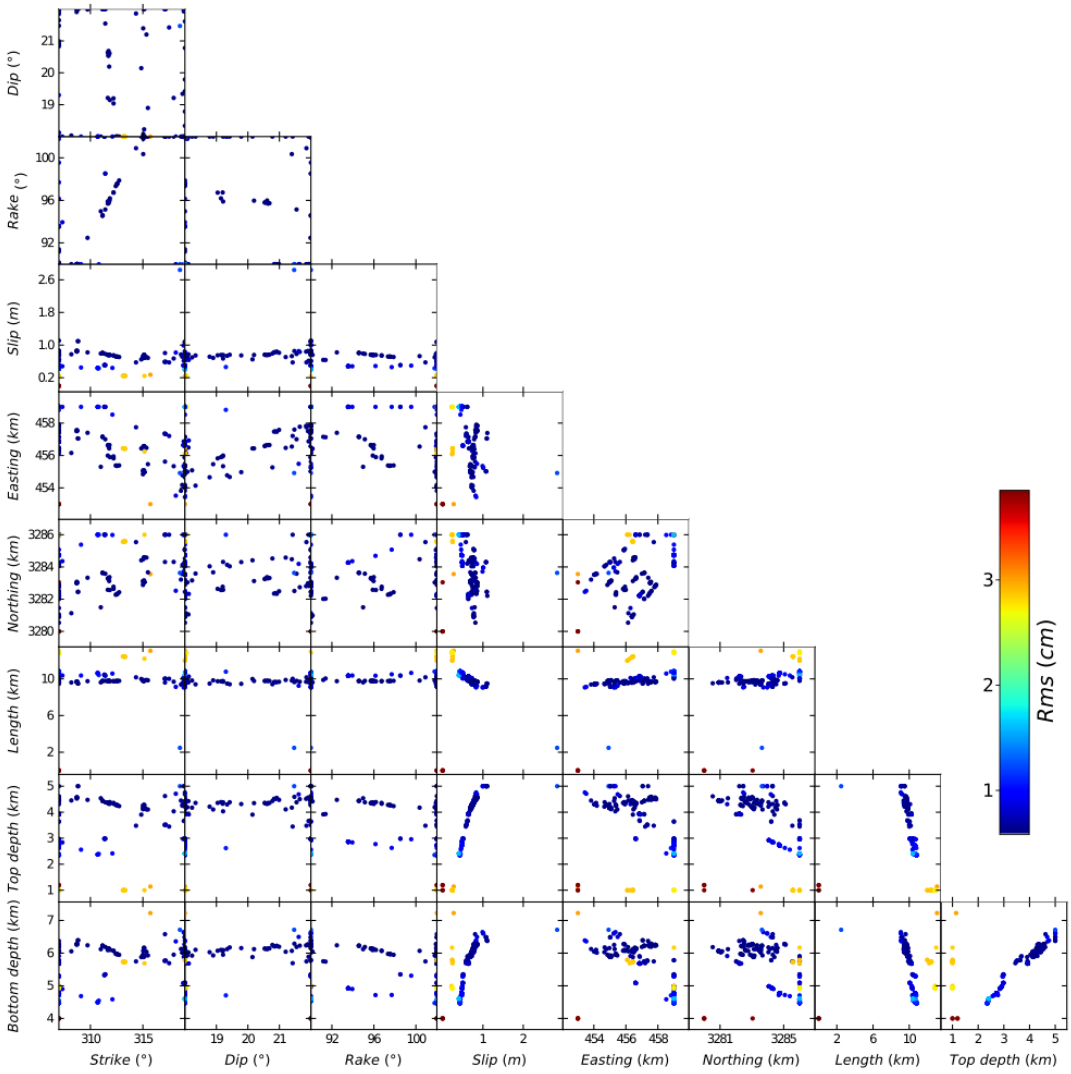

Figure S8, Trade-off between fault parameters for the NE-dipping fault model. Each dot represents the result of the 300 Monte Carlo restart of the uniform inversion. Each dot is colored by the root mean square residual between InSAR data and the model.

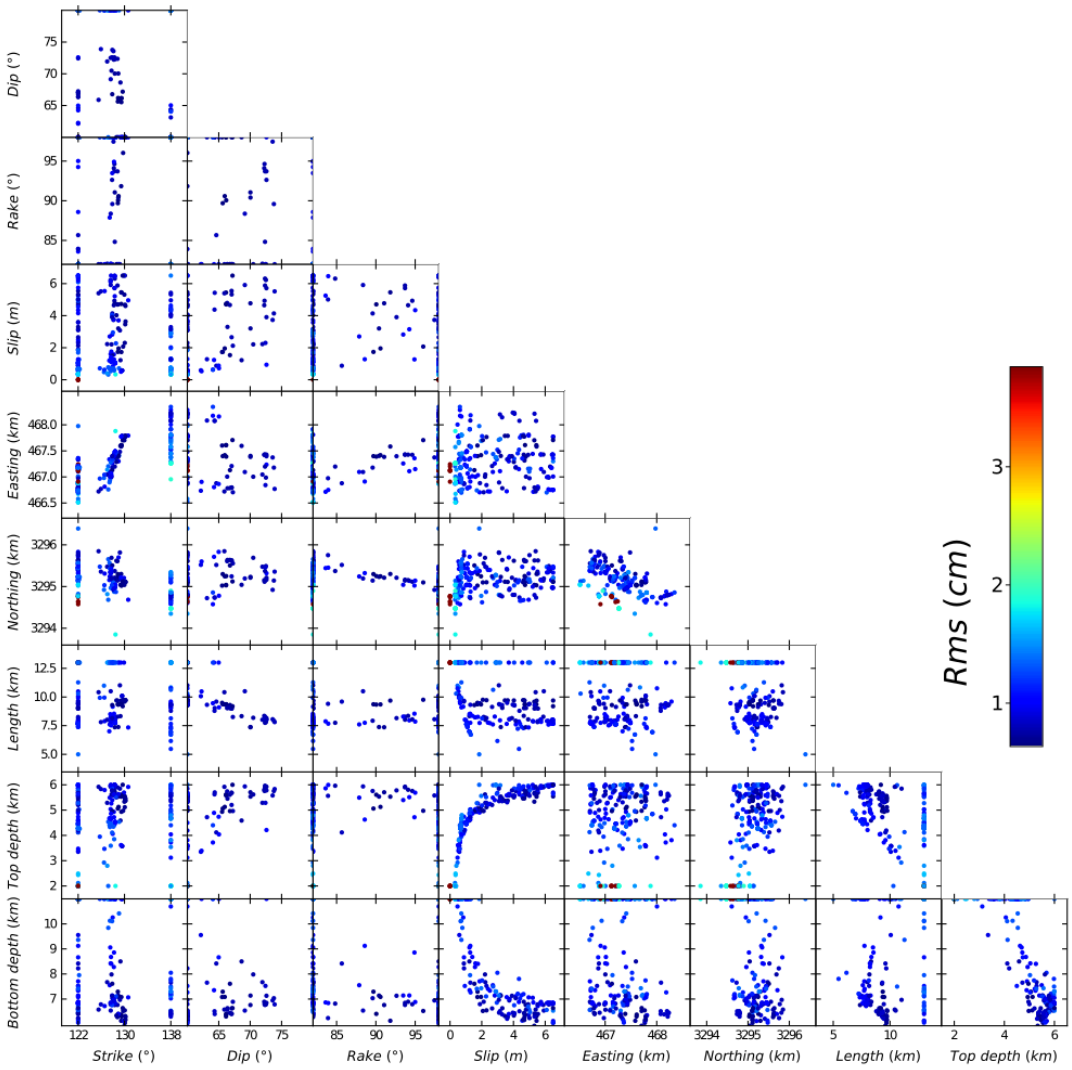

Figure S9, Trade-off between fault parameters for the SW-dipping fault model. See Figure S8 for legend.

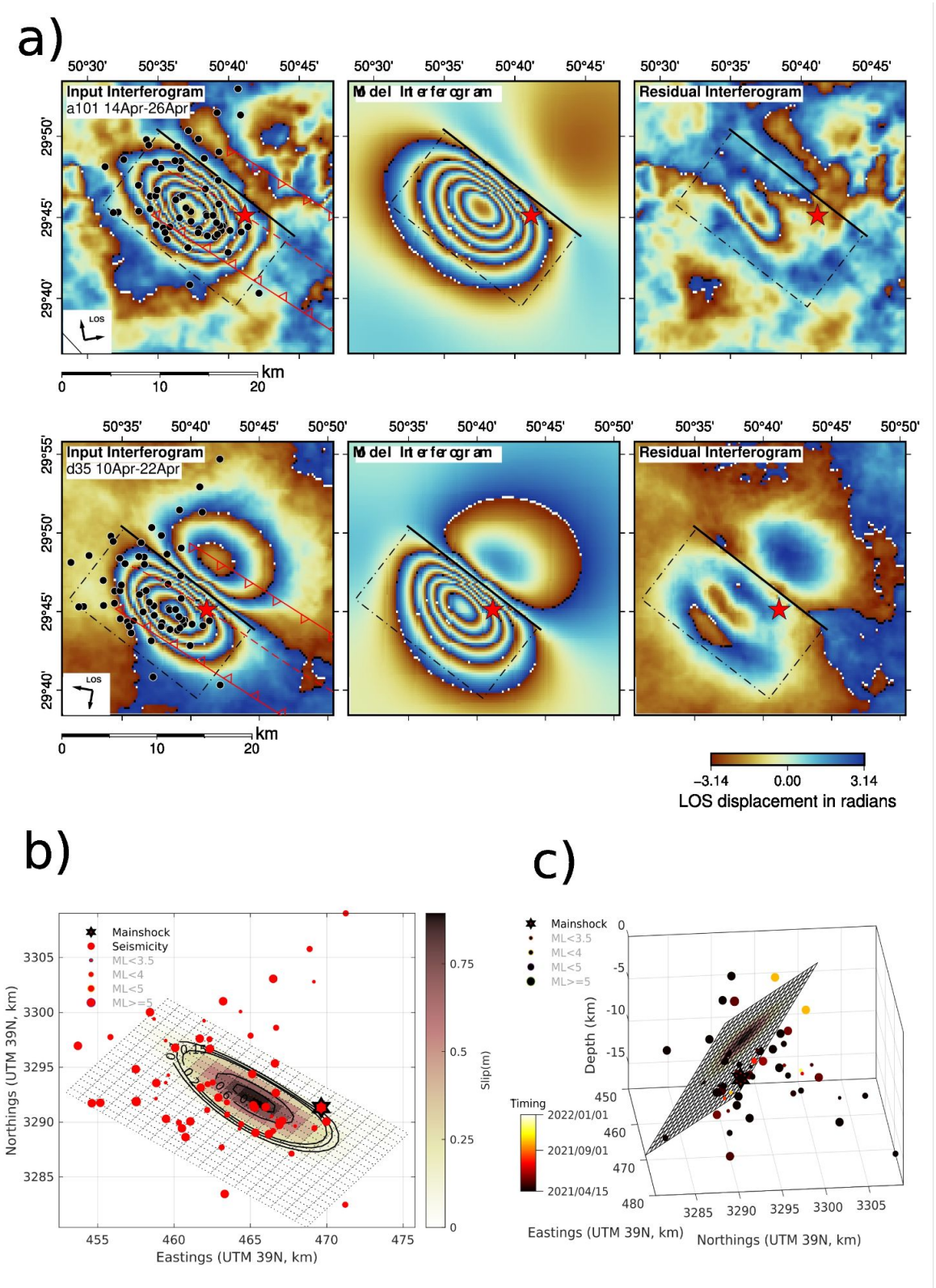

Figure S10, Coseismic slip distribution inversion results for SW-dipping fault model. See figure S5 for the detailed caption. The model yields an RMS of 0.00387 m.

Table S1: Relocated events of the Genaveh seismic sequence. Date and time are given as year.month.day and hour:minute:second.millisecond format. Lat and Lon are epicentral parameters (latitude and longitude) in degrees. Depth is focal depth (km); **c** represents the fixed depth at 12 km and **l** shows the events with resolved depth. The order of events (No) is the same as events number in figure 2b.

No	Date	Time	Lat	Long	Depth	M
1	0	0.19	30.46	50.75	12l	4.2mb
2	0	0.04	30.51	50.67	14l	3.8mb
3	0	0.41	29.58	50.86	8l	3.7mb
4	0	0	30	50.74	9l	4.3mb
5	0	0.6	29.7	51.2	0	4.3mb
6	0	0.12	30.25	51.3	8l	3.9mb
7	0	0.12	29.9	51.34	12l	4.1mb
8	0	0.18	30.45	50.82	14l	3.7mb
9	0	0.79	29.79	50.53	0	3.6mb
10	0	0.76	30.47	50.72	14l	3.9mb
11	0	0.61	29.52	50.89	11l	0
12	0	0.7	29.54	50.93	11l	4.3mb
13	0	0.72	29.52	50.94	12l	3.9mb
14	0	0.74	29.55	50.93	15l	4.2mb
15	0	0.75	29.51	50.93	12l	3.8mb
16	0	0.77	29.55	50.88	8l	3.7mb
17	0	0.78	29.56	50.96	14l	3.8mb
18	0	0.86	29.55	50.93	14l	4.5mb
19	0	0.95	29.55	50.88	12l	3.7mb
20	0	0.11	29.57	50.9	12l	3.8mb
21	0	0.6	29.5	50.93	17l	3.8mb
22	0	0.73	29.53	50.93	14l	3.7mb
23	0	0.73	29.54	50.91	13l	4.1mb
24	0	0.74	29.57	50.91	21l	3.6mb
25	0	0.89	29.53	50.93	12l	3.8mb
26	0	0.73	29.54	50.93	0	3.7mb
27	0	0.02	29.56	50.91	0	4.3mb
28	0	0.03	29.53	50.86	12l	4.2mb
29	0	0.03	29.53	50.88	0	4.3mb
30	0	0.28	29.53	50.94	9l	4.3mb
31	0	0.69	30.43	50.64	14l	4.2mb
32	0	0.7	30.43	50.79	11l	3.8mb
33	0	0.86	29.42	51.08	9l	0
34	0	0.91	29.74	51.19	6l	3.9mb
35	0	0.29	29.9	50.58	14l	3.7mb
36	0	0.57	29.53	51.38	9l	4.2mb
37	0	0.82	29.58	51.41	7l	4.4mb
38	0	0.95	29.67	50.77	15l	3.9mb
39	0	0.19	29.7	50.77	12l	4.9mb
40	0	0.37	30.17	50.9	5l	3.8mb
41	0	0.13	30.2	50.88	6l	0
42	0	0.37	30.37	50.72	13l	4.3mb
43	0	0.59	30.38	50.73	13l	0
44	0	0.41	30.19	51.04	7l	4.2mb

45	0	0.03	29.75	51.35	14l	4.4mb
46	0	0.49	30.43	50.53	0	3.7mb
47	0	0.2	30.21	50.91	12l	4.3mb
48	0	0.28	29.75	50.69	9l	5.8Mw
49	0	0.29	29.74	50.58	4l	4.5mb
50	0	0.29	29.8	50.59	12c	4.2mb
51	0	0.3	29.76	50.54	3l	4.5mb
52	0	0.32	29.74	50.59	12c	3.6ML
53	0	0.33	29.75	50.64	13l	4.5mb
54	0	0.35	29.91	50.7	18l	3.6ML
55	0	0.37	29.86	50.65	16l	4.4mb
56	0	0.38	29.76	50.57	12c	3.3ML
57	0	0.4	29.81	50.61	12l	3.6ML
58	0	0.44	29.88	50.68	12c	3.9ML
59	0	0.47	29.73	50.68	0	3.5ML
60	0	0.68	29.78	50.56	11l	0
61	0	0.91	29.8	50.61	7l	4.4mb
62	0	0.93	29.74	50.66	8l	4.7mb
63	0	0.95	29.76	50.66	15l	4.3mb
64	0	0.95	29.73	50.59	8w	4.4mb
65	0	0.99	29.72	50.62	11l	3.7ML
66	0	0.04	29.76	50.62	0	3.8ML
67	0	0.08	29.75	50.64	14l	4.2mb
68	0	0.12	29.77	50.57	8l	4.2mb
69	0	0.17	29.77	50.58	12l	3.4ML
70	0	0.26	29.74	50.66	7l	0
71	0	0.44	29.75	50.61	0	3.5ML
72	0	0.45	29.75	50.62	18l	3.6ML
73	0	0.49	29.74	50.66	6l	3.5ML
74	0	0.58	29.74	50.63	12c	3.5ML
75	0	0.75	29.77	50.61	12c	3.5ML
76	0	0.9	29.79	50.65	7l	4.3mb
77	0	0.99	29.73	50.63	12c	3.3ML
78	0	0.36	29.73	50.65	12l	4.1mb
79	0	0.71	29.82	50.66	12l	3.5ML
80	0	0.75	29.68	50.62	8l	4.3mb
81	0	0.9	29.71	50.67	0	3.5ML
82	0	0.06	29.86	50.68	12c	3.4ML
83	0	0.11	29.67	50.7	15l	3.6ML
84	0	0.75	29.73	50.65	12l	3.6ML
85	0	0.9	29.73	50.59	12l	0
86	0	0.96	29.81	50.54	11l	3.5ML
87	0	0.41	29.75	50.53	12c	4.1mb
88	0	0.92	29.81	50.64	13l	3.6ML
89	0	0.53	29.74	50.6	14l	4.4mb
90	0	0.15	29.78	50.58	0	3.2ML
91	0	0.67	29.75	50.65	0	4.4mb
92	0	0.68	29.74	50.69	18l	4.6mb
93	0	0.96	29.83	50.63	0	3.3ML
94	0	0.24	29.77	50.6	12l	4.3mb

95	0	0.49	29.76	50.56	5l	0
96	0	0.96	29.74	50.66	14l	2.9ML
97	0	0.4	29.84	50.62	12l	4.5mb
98	0	0.86	29.81	50.6	7l	4.9mb
99	0	0.09	29.73	50.64	15l	4.6mb
100	0	0.21	29.81	50.58	12l	2.7ML
101	0	0.1	29.78	50.64	9l	4.2mb
102	0	0	29.82	50.61	12l	2.7ML
103	0	0.47	29.86	50.89	5l	0
104	0	0.61	29.74	51.19	11l	5.4Mw
105	0	0.88	29.76	50.62	12l	4.2mb
106	0	0.88	29.77	50.61	0	3.5ML
107	0	0.3	29.74	50.67	12l	3.3ML
108	0	0.4	29.89	50.88	6l	4.6mb
109	0	0.5	29.86	50.89	11l	3.9ML
110	0	0.61	29.74	50.65	12l	2.8ML
111	0	0.05	29.8	50.52	4l	4.9Mw
112	0	0.11	29.83	50.57	6l	4.6mb
113	0	0.86	29.82	50.57	13l	2.9ML
114	0	0.38	29.74	51.12	8l	4.3mb
115	0	0.9	29.73	51.15	13l	4.1mb
116	0	0.75	29.7	51.18	9l	0
117	0	0.76	29.67	51.15	12l	4.2mb

Table S2: The crustal model (Moho depth 47 km), to predict theoretical travel times for relocation of the sequence.

Depth (km)	**Vp** (km/sec.)	**Vs** (km/sec.)
0.0	5.8	3.1
20.0	5.8	3.1
20.0	6.4	3.8
47.0	6.4	3.8

Table S3: The detail of focal mechanism solution of the 18 April 2021 Mw 5.9 Genaveh earthquake obtained in this study and other available solution; the Global Centroid Moment Tensor (GCMT), United States Geological Survey (USGS), and the GFZ German Research Centre for Geosciences.

Source	**Date and time (UTC)**	**Latitude°**	**Longitude°**	M_w	**Depth (km)**	**Strike1°**	**Dip1°**	**Rake1°**	**Strike2°**	**Dip2°**	**Rake2°**
GFZ	2021-04-18 06:41:49	29.75	50.67	6.0	14	137	74	97	291	17	64
GCMT	2021-04-18 06:41:50	29.631	50.659	5.9	10	126	64	88	310	26	94
USGS	2021-04-18 06:41:49	29.753	50.678	5.8	12	139	62	95	308	28	80
This study	**2021-04-18 06:41:50**	**29.751**	**50.685**	**5.9**	**6.0 ± 2.0**	**131 ± 5**	**62 ± 4**	**92 ± 5**	**306 ± 5**	**28 ± 9**	**86 ± 10**

Table S4: Moment tensor solutions of the Genaveh earthquake sequence and background events obtained in this study. Table columns refer to the event number, date and time in UTC (yyyy-mm-dd hh:mm:ss), relocated latitude and longitude, Magnitude (Mw), centroid depth, and strikes, dips, and rakes of the two nodal planes with estimated uncertainties.

No	Date and time (UTC)	Latitude°	Longitude°	M_w	Depth (km)	Strike1°	Dip1°	Rake1°	Strike2°	Dip2°	Rake2°
1	2014-05-21 09:46:29	29.604	50.863	5.3	8.0 ± 1.0	119 ± 13	61 ± 3	94 ± 16	291 ± 14	29 ± 5	83 ± 20
2	2014-05-21 10:51:27	29.631	50.859	5.1	6.0 ± 1.0	123 ± 24	67 ± 2	89 ± 46	307 ± 2	23 ± 2	93 ± 2
3	2014-06-20 22:54:18	29.872	50.897	5.0	11.0 ± 2.0	97 ± 56	52 ± 7	37 ± 25	342 ± 14	62 ± 12	135 ± 42
4	2018-03-19 04:30:46	29.696	50.767	5.0	9.0 ± 1.0	130 ± 20	60 ± 5	89 ± 4	310 ± 5	30± 3	90± 4
5	2021-04-18 06:41:50	29.751	50.685	5.9	6.0 ± 2.0	131 ± 5	62 ± 4	92 ± 5	306 ± 5	28 ± 3	86 ± 8
6	2021-04-18 08:50:37	29.857	50.653	4.2	4.0 ± 1.0	129 ± 5	64 ± 3	86 ± 8	318 ± 6	26 ± 3	98 ± 7
7	2021-04-18 21:50:19	29.799	50.610	4.1	5.0 ± 1.0	122 ± 7	75 ± 6	88 ± 8	309 ± 8	15 ± 6	96 ± 12
8	2021-04-18 22:17:45	29.737	50.657	4.6	6.0 ± 1.0	135 ± 4	60 ± 2	94 ± 6	307 ± 4	30 ± 1	83 ± 4
9	2021-04-18 22:43:50	29.727	50.594	4.2	6.0 ± 1.0	320 ± 9	68 ± 6	93 ± 13	133 ± 9	22 ± 6	83 ± 12
10	2021-04-19 21:32:47	29.788	50.6543	4.0	6.0 ± 1.0	257 ± 10	69 ± 11	-68 ± 14	28 ± 11	30 ± 10	-135 ± 15
11	2021-04-20 17:55:27	29.680	50.620	4.2	4.0 ± 1.0	306 ± 6	47 ± 10	88 ± 9	129 ± 8	43±11	92 ± 8
12	2021-05-07 12:44:50	29.740	50.597	4.1	12.0 ± 2.0	94 ± 5	55 ± 2	68 ± 8	309 ± 4	40 ± 2	117 ± 4
13	2021-05-12 16:26:14	29.740	50.689	4.3	6.0 ± 1.0	134 ± 6	62 ± 4	92 ± 7	309 ± 6	28 ± 4	86 ± 8
14	2021-05-21 11:52:15	29.756	50.560	5.0	4.0 ± 1.0	310 ± 3	45 ± 2	88 ± 2	134 ± 3	45 ± 2	92 ± 3
15	2021-05-28 20:35:48	29.808	50.603	4.9	4.0 ± 1.0	307 ± 9	56 ± 11	80 ± 21	144 ± 20	35 ± 11	104 ± 21
16	2021-05-29 00:55:02	29.805	50.643	4.0	8.0 ± 1.0	293 ± 13	70 ± 3	68 ± 16	163 ± 14	29 ± 5	135 ± 20
17	2021-05-29 02:12:53	29.731	50.641	4.7	6.0 ± 1.0	287 ± 24	65 ± 2	56 ± 46	165 ± 2	41 ± 2	140 ± 2
18	2021-05-29 02:17:17	29.756	50.583	4.1	7.0 ± 2.0	298 ± 56	53 ± 7	78 ± 25	137 ± 14	38 ± 12	105 ± 42
19	2021-05-29 23:02:50	29.713	50.578	4.0	8.0 ± 1.0	292 ± 20	48 ± 5	95 ± 4	105 ± 5	42 ± 3	84 ± 4
20	2021-07-13 11:11:49	29.862	50.893	4.9	3.0 ± 1.0	131 ± 5	55 ± 4	96 ± 5	300 ± 5	35 ± 3	81 ± 8
21	2021-07-18 14:34:17	29.737	50.189	5.6	9.0 ± 1.0	119 ± 5	57 ± 3	85 ± 8	308 ± 6	33 ± 3	98 ± 7
22	2021-07-29 23:47:24	29.678	50.567	4.4	4.0 ± 1.0	132 ± 7	55 ± 6	106 ± 8	285 ± 8	38 ± 6	68 ± 12
23	2021-08-13 09:31:27	29.886	50.882	4.4	4.0 ± 1.0	302 ± 4	42 ± 2	83 ± 6	131 ± 4	48 ± 1	96 ± 4
24	2021-10-01 02:33:19	29.829	50.569	4.3	8.0 ± 2.0	120 ± 9	72 ± 6	103 ± 13	262 ± 9	22 ± 6	55 ± 12
25	2021-12-14 09:12:53	29.735	51.121	4.1	12.0 ± 2.0	230 ± 10	84 ± 11	-15 ± 14	322 ± 11	75 ± 10	-173 ± 15

Table S5: InSAR model source parameters from uniform slip inversion. Eastings and Northings in km are the center of the projected surface break (UTM 39). The difference between the columns depends on the slip parameter being fixed or not.

Parameters	**NE-dipping fault**		**SW-dipping fault**	
Strike (°)	313	311	128	128
Dip (°)	19	20	59	66
Rake (°)	100	96	94	90
Slip (m)	0.5 (fixed)	0.76	0.5 (fixed)	4.7
Eastings (km)	457.1	456.6	467.4	467.4
Northings (km)	3284.6	3283.2	3295.1	3295.2
Length (km)	10.7	9.8	10.8	9.3
Top depth (km)	3.3	4.3	3.1	5.6
Bottom depth (km)	5.5	6.1	9.9	6.4
Moment (Nm)	1.1×10^{18} (Mw 5.98)	0.8×10^{18} (Mw 5.92)	1.0×10^{18} (Mw 5.95)	0.9×10^{18} (Mw 5.92)
RMS (m)	6.89×10^{-3}	5.79×10^{-3}	8.85×10^{-3}	6.32×10^{-3}